Biochemical Pharmacology 78 (2009) 1167–1177

Contents lists available at ScienceDirect

Biochemical Pharmacology

journal homepage: www.elsevier.com/locate/biochempharm

Interference with endothelial cell function by JG-03-14, an agent that binds to the colchicine site on microtubules☆

Nava Dalyot-Herman [a], Fernando Delgado-Lopez [a], David A. Gewirtz [b], John T. Gupton [c], Edward L. Schwartz [a,*]

[a] Department of Oncology, Albert Einstein College of Medicine, Bronx, NY 10467, United States
[b] Department of Pharmacology and Toxicology and Massey Cancer Center, Virginia Commonwealth University, Richmond, VA, United States
[c] Department of Chemistry, University of Richmond, Richmond, VA, United States

ARTICLE INFO

Article history:
Received 16 March 2009
Accepted 23 June 2009

Keywords:
JG-03-14
Microtubule-binding drugs
Angiogenesis inhibitors
Vascular-disrupting drugs
VE-cadherin

ABSTRACT

JG-03-14, a novel tetrasubstituted pyrrole with microtubule-depolymerizing and anti-proliferative activities, was tested for its effect on endothelial cell (EC) functions *in vitro*. JG-03-14 was a potent inhibitor of EC vessel-like tube formation on extracellular matrix (IC_{50} of 40 nM) and caused the involution of established vessels, potential anti-angiogenic and vascular-disrupting activities, respectively. These actions were not due to the inhibition of EC proliferation or to the induction of apoptosis by JG-03-14. While similar effects were observed with the microtubule-depolymerizing and vascular-disrupting drug combretastatin-A4 (CoA4), JG-03-14 had a more selective effect on tube formation, relative to its cytotoxic actions, than did CoA4. Potential molecular mechanisms for JG-03-14's anti-vascular actions were explored. In contrast to the taxanes, which also have anti-vascular actions, JG-03-14 did not disrupt focal adhesion formation or block VEGF-induced phosphorylation of focal adhesion kinase. It did, however, inhibit VEGF-induced phosphorylation of VE-cadherin and reduce the association of β-catenin with VE-cadherin. It caused cell retraction, intercellular gaps, and abnormally elongated adherens junctions at low concentrations, and prominent, but reversible, plasma membrane blebbing at higher concentrations. These results suggest that JG-03-14 may affect vascular morphogenesis by disrupting the interaction of adjacent endothelial cells, possibly as a consequence of effects on VE-cadherin, β-catenin, and/or actin. They also provide the first report of anti-vascular activity for this class of compounds.

1. Introduction

The broad clinical anti-tumor efficacy of paclitaxel, docetaxel and the vinca alkaloids have prompted studies to identify and design drugs that bind to, and interfere with, the function of microtubules [1]. Microtubules are essential elements of the cytoskeleton that are important in mitosis, cell division, and in a number of processes in interphase cells. Although they are thought to act clinically predominantly by their direct cytotoxic actions on tumor cells, more recent studies have demonstrated that most microtubule-binding drugs have anti-angiogenic and vascular-disrupting actions in a variety of *in vivo* assays, including those measuring neovascularization in subcutaneous matrigel plugs, chick embryo chorioallantoic membranes, corneal micropockets, and tumor xenografts [2–8]. It is noteworthy that a number of *in vitro* anti-vascular actions of the microtubule-binding drugs occur at concentrations that are substantially lower than those at which the drugs block mitosis, produce cell cycle arrest or induce apoptosis [5–8]. These observations have prompted the search for microtubule-related drug actions that may have greater selectivity for the vasculature, and which would provide additional targets for the development of microtubule-binding drugs.

Tumor neovascularization occurs primarily through the sprouting of established vessels, a process that includes the migration of endothelial cells (EC) out of an existing vessel into the surrounding extracellular matrix (ECM) and their organization and morphogenesis into tube-like structures, processes that may be accompanied by an increase in proliferation [9]. Agents which interfere with these events will potentially have anti-angiogenic activity. Those agents whose actions also include acute effects on cell shape and cell–cell junctions can additionally cause vascular disruption, characterized *in vivo* by the rapid collapse of tumor blood flow and an increase in permeability of the vasculature to macromolecules

☆ Grant support: NCI/NIH grants RO1 CA98456 and RO1 CA89352 (E.L. Schwartz).
Abbreviations: CoA4, combretastatin A4; Col, colchicine; EC, endothelial cell; ECM, extracellular matrix; FAK, focal adhesion kinase; VEGF, vascular endothelial growth factor.

* Corresponding author at: Department of Oncology, Albert Einstein College of Medicine, Montefiore Medical Center, 111 East 210th Street, Bronx, NY 10467, United States. Tel.: +1 718 920 4015; fax: +1 718 882 4464.
E-mail address: eschwart@aecom.yu.edu (E.L. Schwartz).

0006-2952/$ – see front matter © 2009 Elsevier Inc. All rights reserved.
doi:10.1016/j.bcp.2009.06.093

[10]. Aspects of these processes can be studied in tissue culture. When plated on ECM, endothelial cells form structures which morphologically resemble capillary-like vessels, with lumens and an anastomosing and branching tubular network [11]. Time-lapse photography has shown that EC vessel network formation is a dynamic process involving cell migration and frequent cell–matrix and cell–cell interactions [12]. These interactions are mediated by several endothelial cell surface adhesion molecules which include the integrins (cell–ECM interactions) and the cadherins (homotypic cell–cell interactions [13,14].

Colchicine was one of the first agents to be shown to bind to tubulin protein, where it inhibits microtubule polymerization and causes the loss of cellular microtubules [15]. Early studies found that cell locomotion was blocked when fibroblasts were treated with colchicine, and subsequent studies suggested several mechanisms by which the dynamic growth and shortening of microtubules may directly or indirectly regulate cell migration [16,17]. Despite having anti-proliferative and anti-vascular actions in experimental models, colchicine has not been found to be clinically useful as an anti-cancer agent, in contrast to members of the vinca (also microtubule destabilizers) and taxane (microtubule stabilizers) classes of microtubule-binding drugs [1]. More recently, several small molecules with diverse chemical structures that bind to the colchicine site on microtubules have been shown to have anti-tumor efficacy in ongoing clinical trials, including 2-methoxyestradiol, combretastatin A4 (CoA4), several CoA4 analogs, and a number of methoxybenzene–sulfonamide compounds [10,18–21].

The current investigation was designed to characterize the actions of the substituted pyrrole, 3,5-dibromo-4-(3,4-dimethoxyphenyl)-1H-pyrrole-2-carboxylic acid ethyl ester (JG-03-14; Fig. 1A), on endothelial cell function [22]. Natural products containing a pyrrole have diverse biological actions, and have been useful as lead compounds for drug development [23,24]. While JG-03-14 has been shown to have broad cytotoxic and anti-proliferative effects against cancer cells line *in vitro* and to inhibit tumor growth *in vivo*, its ability to potently bind at or near the colchicine site on tubulin prompted the present investigations [24,25]. Molecular modeling studies have indicated that while the dimethoxyphenyl group of JG-03-14 occupies a space similar to that of the trimethoxyphenyl group of colchicine, the tetrasubstituted pyrrole group interacted with both α- and β-tubulin in space not shared with colchicine, suggesting significant differences compared with colchicine in the mechanism of binding to tubulin [24]. We found that JG-03-14 had direct effects on endothelial cells that could be indicative of therapeutically useful anti-vascular actions.

2. Materials and methods

2.1. Drugs and cell culture

JG-03-14 was synthesized as previously described [22]; combretastatin A4 and colchicine were from Tocris Biosciences (Ellisville, MO) and Sigma (St. Louis, MO), respectively. All other reagents were from Sigma, except when noted. Stock solutions of the drugs were prepared in DMSO and stored at −20 °C. HMEC-1 human microvascular endothelial cells [26] were cultured in MCDB131 medium containing 10% fetal bovine serum (Invitrogen, Carlsbad, CA), 10 ng/ml endothelial growth factor, 1 μg/ml hydrocortisone, 1% penicillin/streptomycin, and 5 mM L-glutamine. Human umbilical vein endothelial cells (HUVEC, Cascade Biologics, Portland, OR) were cultured in medium M200 (Cascade Biologics) with low serum growth supplement (Cascade Biologics) and penicillin/streptomycin (Invitrogen). Cells were cultured at 37 °C in a humidified atmosphere with 5% CO_2.

2.2. Cell attachment to extracellular matrix

Cells were treated with drug for 24 h, washed, trypsinized, and then plated (5×10^4 endothelial cells per well) in quadruplicate on a 96 well plate which had been pre-coated with collagen type I and blocked with 0.1% BSA in PBS. Cells were allowed to attach for 20 min at 37 °C, at which time media with unattached cells were gently aspirated and the wells were washed 3× with PBS. Attached cells were fixed with 10% TCA and incubated 1 h in cold. The cells were stained with sulforhodamine B (SRB; 0.4% in 1% acetic acid) and incubated at room temperature for 30 min. The plate was rinsed 4× with 1% acetic acid and dried. The SRB was dissolved by adding 10 mM Tris-base. Absorbances were read at 510 nm on plate reader.

2.3. Cell proliferation, apoptosis, and necrosis assays

Cells were seeded in 96 well plates in quadruplicate (5×10^3 well^{-1}) and allowed to attach for 24 h before different concentrations of the drugs were added for an additional 48 or 72 h. The degree of proliferation was then quantitated by the SRB assay, as described above. Apoptosis was measured after 1 or 24 h of drug treatment using TUNEL *in situ* detection assays (TACS-2, Trevigen, Gaithersberg, MD, or TMR-red, Roche Applied Science, Indianapolis, IN). Cell necrosis was assessed by staining cells with propidium iodide (10 μg/ml in medium) for 30 min.

2.4. Immunofluorescence and F-actin visualization

Cells were grown in four chamber slides for 24 h before the drugs were added for an additional 24 h. In some experiments, cells were treated with drug for 1.5 h, washed, and drug-free medium was added for an additional 22.5 h. Immediately after treatment, cells were fixed in freshly prepared 3.4% paraformaldehyde in PBS for 10 min, washed twice with PBS, permeabilized with 0.2% Triton X-100 in PBS, blocked with 5% BSA in PBS for 1 h, and then incubated overnight with mouse anti-alpha-tubulin (1:300) in 1% BSA, PBS, 0.1% Triton X-100 at 4 °C. After three washes with PBS, cells were incubated with Alexa Fluor 488 rabbit anti-mouse IgG (Invitrogen; 1:300) for 1 h at RT. For F-actin visualization, the cells were permeabilized as above and incubated with 0.35 μg/ml of phalloidin-tetramethylrhodamine B isothiocyanate conjugate (Fluka, Ronkonkoma, NY) for 1 h. For immunofluorescent visualization of VE-cadherin, the fixed cells were directly incubated with a rabbit anti-VE-cadherin antibody (Invitrogen) for 1 h. For immunofluorescence of FAK, the fixed cells were washed and permeabilized with 0.5% Triton X-100. The cells were treated for 1 h with blocking buffer (1% BSA, 0.1% Tween 20 in PBS) before incubating with rabbit anti-FAK antibody (Santa Cruz Biotechnology, Santa Cruz, CA). Slides were washed after the first antibody and incubated with a FITC-conjugated secondary antibody for 1 h, and were mounted with SlowFade Gold antifade reagent with DAPI (Invitrogen). Images were obtained on a fluorescent microscope (Olympus) equipped with a digital camera (SPOT RT, Diagnostic Instruments).

2.5. Assessment of microtubule sensitivity to drug-mediated disassembly

A differential extraction procedure to separate detergent-soluble and -insoluble tubulin was used to assess the sensitivity of endothelial cell microtubules to disassembly by the drugs, as previously described [27]. Cytoplasmic microtubules remain polymerized and insoluble when cells are lysed rapidly at a warm

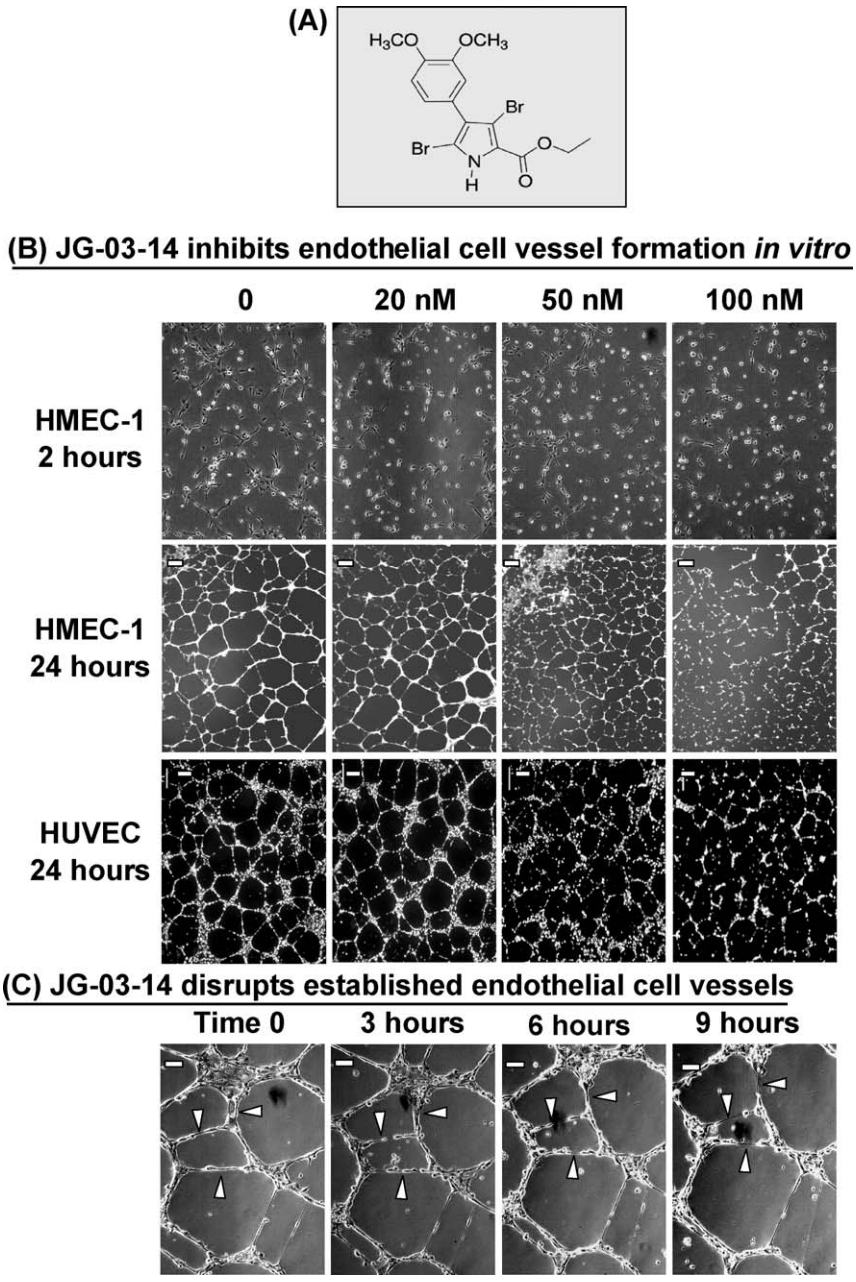

Fig. 1. (A) Structure of 3,5-dibromo-4-(3,4-dimethoxyphenyl)-1H-pyrrole-2-carboxylic acid ethyl ester (JG-03-14). (B) JG-03-14 inhibits endothelial cell tube formation *in vitro*. HMEC-1 or HUVEC endothelial cells were plated on Matrigel-coated wells with media alone or with the indicated concentrations of JG-03-14 for 2 or 24 h. The cells were fixed and stained with phalloidin-tetramethylrhodamine B isothiocyanate conjugate (HMEC-1; 24 h) or with calcein AM (HUVEC; 24 h). Bar = 200 μm. (C) After allowing HMEC-1 cells to form vessels on Matrigel for 24 h, 100 nM JG-03-14 was added to the media. The same microscopic field was recorded every 3 h thereafter. Arrowheads indicate vessels which degenerated with time. Bar = 20 μm.

temperature and in a PIPES–EGTA-based buffer containing detergent [28]. Confluent cells in 12 well plates were treated with the drugs for 2 h. The cells were washed with warm (37 °C) PBS and incubated with 100 μl warm lysis buffer (80 mM PIPES-KOH, pH 6.8, 1 mM $MgCl_2$, 1 mM EGTA, 0.2% Triton X-100, 10% glycerol and protease inhibitor cocktail) for 3 min. Lysates containing detergent-soluble proteins were carefully removed and mixed with Laemelli loading buffer. To obtain the polymerized tubulin from the insoluble fraction, 100 μl of 1% SDS in water was added to the wells. The plates were scraped and the extracts were sonicated for 15 s. The lysate was centrifuged and the supernatant was mixed with Laemelli loading buffer. Equal volumes of soluble and insoluble proteins were boiled and analyzed by 7.5% PAGE, followed by immunoblotting with anti-α-tubulin and β-tubulin antibodies.

2.6. Migration by wound healing assay

Cells were allowed to grow to full confluency in 24 well plates. The cells were mechanically "wounded" by scraping with a pipette tip, denuding a strip of the monolayer 300 μm wide. The cells were rinsed with PBS to remove dislodged cells and cellular debris. Media containing the drugs at different concentrations was added and the "wound" was observed 24 h later with an inverted microscope (Olympus). The recovery of each denuded area was quantified by measuring the gap at time "0" and 24 h

following the drugs addition, and calculating the percent of gap closure.

2.7. Endothelial cell vessel formation on Matrigel matrix

Matrigel (BD Biosciences, Bedford, MA) was added to 24 well plates and allowed to gel at 37 °C for 30 min. The gels were overlaid with 1 ml of medium containing 1×10^5 cells and different concentrations of the drugs. The effect of the drugs on capillary tube formation was inspected at time points up to 24 h by inverted light microscopy. Alternatively, the cells were fixed with 4% paraformaldehyde, permeabilized with 0.2% Triton X-100 and stained with phalloidin-tetramethylrhodamine B isothiocyanate conjugate or with calcein AM (both Invitrogen). Vessels were observed with a fluorescent microscope, and vessel formation was quantitated by measuring tube area using Image J software.

2.8. Western blot

Cell extracts were prepared in cold lysis buffer (50 mM Tris pH 7.5, 100 mM NaCl, 50 mM NaF, 5 mM EDTA, 1% Triton X100, 200 μM Na orthovanadate and protease inhibitor cocktail). Protein concentrations were determined using the Bradford reagent (Bio-Rad, Hercules, CA), and normalized cell lysates were mixed with sample buffer (Bio-Rad) containing 2-mercaptoethanol and boiled for 5 min. The samples were run on SDS-polyacrylamide gels and transferred to nitrocellulose membranes. The membranes were incubated overnight with primary antibodies in TBS-T buffer containing 5% BSA: rabbit anti-phospho-FAK [pY^{397}] (BioSource, Camarillo, CA), rabbit anti-phospho-VE-cadherin [pY^{658}] (BioSource), rabbit anti-FAK (Santa Cruz), rabbit anti-VE-cadherin (Invitrogen). After washing, the membranes were incubated with HRP-conjugated secondary antibody for 1 h. The bands were detected with enhanced chemiluminescence reagent (Pierce, Rockford, IL). The intensity of the bands was quantified using Image J software.

2.9. Immunoprecipitation of VE-cadherin and western blotting with β-catenin

HMEC-1 were grown to confluency in 10 cm dishes. The cells were treated with the drugs for 24 h, washed and lysed in 1 ml ice-cold lysis buffer (150 mM NaCl, 50 mM Tris 7.4, 0.5% Triton X-100, 10 mM EGTA 10% glycerol) containing protease inhibitors. The protein concentrations were determined and the lysates were first cleared by incubation for 1 h with protein A/G-agarose beads (Santa Cruz Biotechnology), and then incubated with rabbit antibody against VE-cadherin (1 μg, Invitrogen) or with anti-rabbit IgG as a negative control. After 1 h, fresh protein A/G agarose and 0.1% BSA was added. After incubating overnight at 5 °C, the beads were sedimented by brief centrifugation and washed by resuspending and pelleting four times with 1 ml ice-cold wash buffer (300 mM NaCl, 50 mM Tris–HCl pH 7.4, 0.5% Triton X-100, 10 mM EGTA, 1 mM DTT). The agarose beads were resuspended in 20 μl sample buffer, boiled for 5 min, collected by centrifugation and fractionated on 7.5% SDS-polyacrylamide gel and processed for immunoblotting with a mouse anti-β-catenin antibody (Invitrogen).

2.10. Cell permeability assay

2.5×10^5 HMEC-1 were seeded on transwell filters (3.0 μm pore size, 6.5 mm diameter, Costar) pre-coated with fibronectin in the upper wells of a Boyden chamber, and allowed to grow to confluency for 72 h. The cells were then incubated with the drugs for 24 h. The media in the upper chamber was replaced with fresh media containing 10 μg/ml FITC-labeled dextran (40 kDa). Aliquots from the lower chamber were collected at different time points over the course of 1 h, diluted 1:10, and the fluorescence measured on a SpectroMax M2 microplate reader (Molecular Devices) using excitation/emission wavelengths of 494/521 nm.

2.11. Statistical analyses

Statistical analyses were done with one-way ANOVA, and comparisons were done using Tukey's multiple comparison test. $P < 0.05$ was considered significant.

3. Results

3.1. JG-03-14 inhibits endothelial cell tube formation and disrupts pre-established vessels in vitro

When plated as a monolayer on Matrigel, endothelial cells become elongated and spindle shaped, form tightly adherent cords of cells, and organize into networks of branching and anastomosing tube-like vessels (Fig. 1B). Agents which inhibit these processes may possess potentially clinically useful anti-angiogenic activity. JG-03-14 caused a concentration-dependent inhibition of tube formation with both HMEC-1 microvascular endothelial cells and HUVEC primary endothelial cells, primarily due to the failure of treated cells to undergo the required organizational and morphological changes (Fig. 1B). Inhibition was observed after only 2 h of drug treatment, when vessels were still in the early process of formation, and was prominent at 24 h at concentrations of 50 nM JG-03-14. Several approaches were used to quantitate the inhibition of vessel formation, including direct counting of the number of branched tubes containing two or more junction points under low power magnification, and image analysis of fluorescently labeled (either with phalloidin or calcein AM) cells using Image J to assess vessel length. These methods gave identical results, with a calculated IC_{50} of 40 nM observed for the inhibition of vessel formation in both HMEC-1 and HUVEC.

To evaluate its potential vascular-disrupting actions, the effect of JG-03-14 on pre-established vessels was then tested. The drug was added after the microvessels had formed for 24 h, and the same vessels were then observed every 3 h thereafter. As shown in Fig. 1C (arrows), after a 3 h incubation with 100 nM JG-03-14, some of the pre-established vessels were disrupted, and after 9 h they appeared to be undergoing involution.

3.2. JG-03-14 inhibits endothelial cell migration at non-cytotoxic concentrations

Tube formation *in vitro* requires both cell attachment to ECM and cell migration. Cell motility was assessed with a scratch assay, in which migration is initiated in a confluent layer of cells by mechanical denuding. As can be seen in Fig. 2A, after 24 h control cells had migrated to nearly completely fill in the area that was initially scraped free of cells. This was inhibited by JG-03-14 in a concentration-dependent manner, with an IC_{50} calculated to be 130 nM (Fig. 2A and C). The inhibition of migration by JG-03-14 was not due to the drug causing the detachment of the cells from the matrix; in fact, the ability of cells to attach to ECM was modestly increased by JG-03-14 (Fig. 2C). The effect of JG-03-14 on tube formation and migration was also not due to its anti-proliferative actions: JG-03-14 inhibited proliferation at concentrations (IC_{50} of 240 nM) that were higher than required for the inhibition of migration or tube formation (Fig. 2C). Furthermore, cell proliferation is not required for either the restoration of a confluent cell monolayer in the scrape assay, nor to the formation of tubes on Matrigel. Similar inhibitory effects on cell proliferation

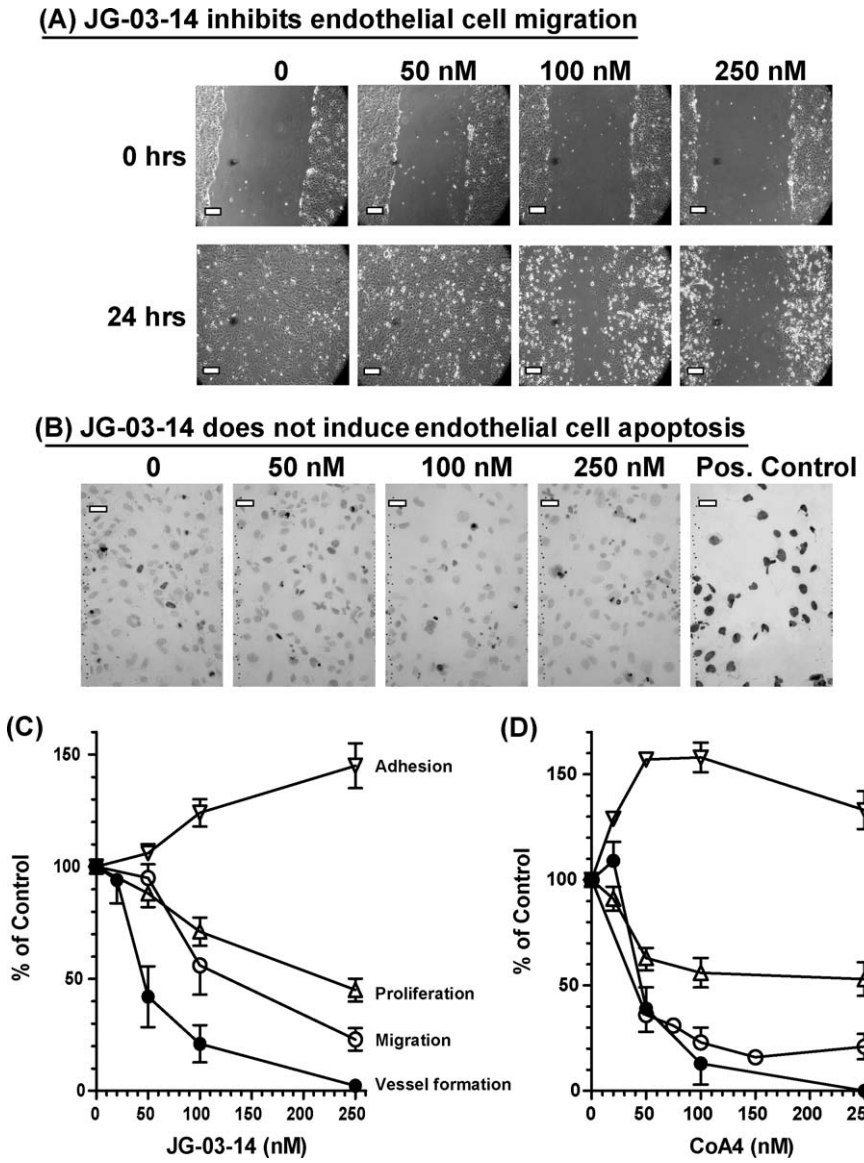

Fig. 2. JG-03-14 inhibits endothelial cell migration and tube formation at non-cytotoxic concentrations. (A) Confluent HMEC-1 cultures were scraped with a pipette tip and then incubated with media only or with the indicated concentrations of JG-03-14. The cultures were photographed just before drug addition (0 h) and after 24 h of drug treatment. Bar = 50 μm. (B) HMEC-1 cells were plated on slides and incubated with the indicated concentrations of JG-03-14 for 24 h. The cells were fixed and assayed for apoptosis using a TACS-2 TUNEL assay kit. The positive control cells were treated identically except for the addition of nuclease immediately prior to staining. Dark-staining cells in the culture indicated apoptotic or necrotic cells. Bar = 100 μm. (C and D) Quantitation and comparison of drug effects on cell adhesion (▽), proliferation (△), migration (○), and vessel formation (●) in HMEC-1 cells in the presence of JG-03-14 (C) and CoA4 (D). Proliferation was quantified after 72 h of drug treatment, as described in Section 2. Migration was quantitated by measuring the gap closure after 24 h of drug treatment, as shown in (A). Tube formation was quantified after 24 h of drug treatment by Image J analysis of the cultures as in Fig. 1B. Attachment was determined by first incubating cells with the drugs for 24 h. The cells were washed and trypsinized and seeded on collagen I pre-coated 96 well plates in quadruplicate in fresh drug-containing media. After 20 min, unattached cells were removed by gentle washing in warm PBS, and the number of attached cells was quantified by the SRB assay. Data are means ± SEM of 5 (panel C) or 2 (panel D) experiments, and are presented as percent of control without drug.

were observed when the HMEC-1 were treated continuously with the drug for 72–96 h, or when they were treated for 24 h (corresponding to the lengths of drug treatment in the tube formation, attachment, and scrape assays), washed free of drug, and were then followed for an additional 72 h (data not shown). Notably, no inhibition of cell proliferation was observed at 50 nM JG-013-14, a concentration that inhibited microvessel formation on Matrigel by approximately 50%.

To role out the possibility that migration and tube formation were inhibited due to the cytotoxicity of the drug, induction of apoptosis in drug-treated HMEC-1 was assessed using an *in situ* TUNEL assay. The results, shown in Fig. 2B, indicated that cells treated with JG-03-14 for 24 h did not undergo apoptosis, even at a concentration of 250 nM. Similar results were obtained with staining the treated cells with trypan blue (data not shown). Since HMEC-1 are immortalized cells and could be resistant to the induction of apoptosis, we also examined the effect of JG-03-14 on HUVEC, which are primary endothelial cells. As shown in the upper panel of Fig. 3 (panels F–H), the drug did not induce apoptosis in HUVEC at concentrations that completely inhibited tube formation. Similarly, no apoptosis was seen at concentrations (1 μM for 1.5 h; Fig. 3I) that caused dramatic changes in cell morphology (see below). The JG-03-14-treated HUVEC were also stained with propidium iodide to detect cell necrosis, a nonspecific final stage of cell death that occurs subsequent to other mechanisms of cell death induction. No significant increase in cell necrosis was

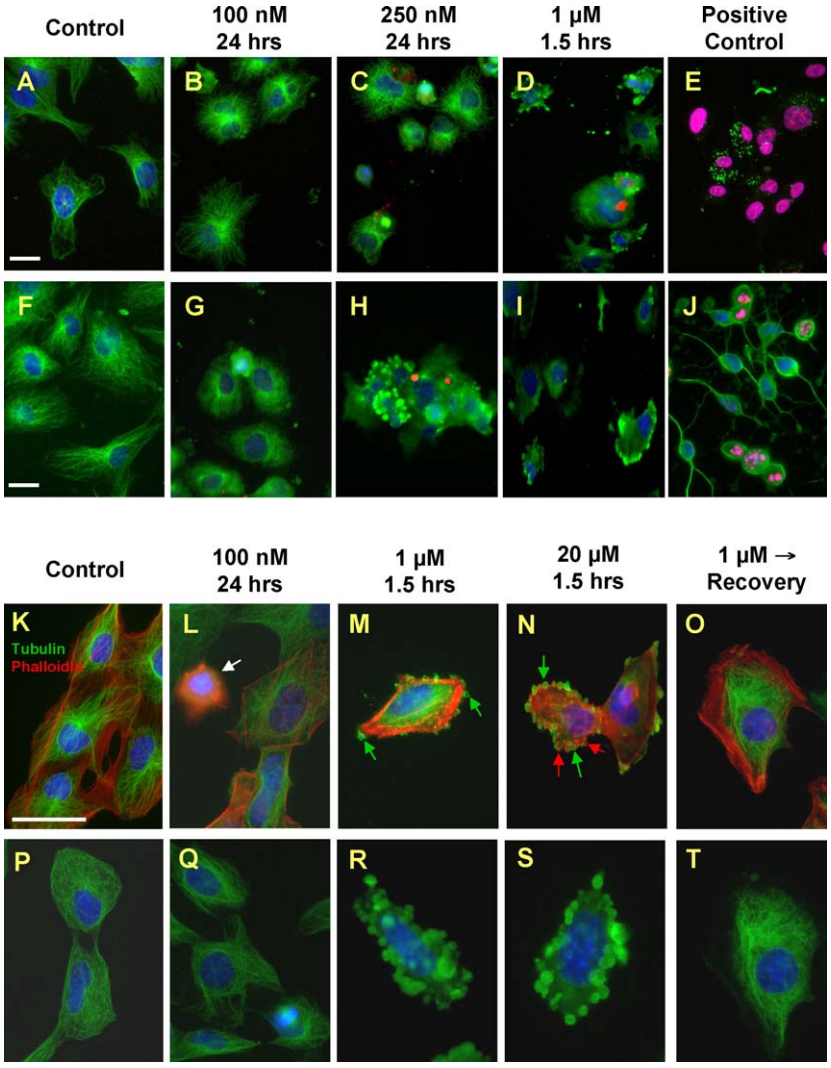

Fig. 3. JG-03-14 induced retraction of endothelial cells and caused blebbing at concentrations that did not induce apoptosis or cause necrosis. HUVEC (panels A–J) and HMEC-1 (panels K–T) cells were treated as follows: (A, F, K and P) medium only; (B, G, L and Q) 100 nM JG-03-14 for 24 h, (C and H) 250 nM JG-03-14 for 24 h, (D, I, M and R) 1 μM JG-03-14 for 1.5 h, (N and S) 20 μM JG-03-14 for 1.5 h, (O and T) 1 μM JG-03-14 for 1.5 h flowed by drug-free medium for 22.5 h. For the positive control in panel (E), cells were treated with 0.1% Triton X-100 for 30 min; in panel (J), cells were treated with 1 μM staurosporine for 30 min. Cells in panels (A–E) were stained with propidium iodide (10 μg/ml for 30 min); cells in panels (F–J) with a TUNEL *in situ* apoptosis kit (TMR red). Cells in panels (K–O) were co-stained with phalloidin-rhodamine (red) and with an antibody to α-tubulin (green); cells in panels (P–T) were only stained for tubulin. Bars = 20 μm. White arrow indicates contracted cells with a dense band of actin; green and red arrows indicate blebs containing tubulin and actin, respectively. Data are representative of several experiments.

observed in HUVEC after JG-03-14 (Fig. 3A–D). Also illustrated in Fig. 3 are positive controls for apoptosis (Triton X-100; Fig. 3J) and necrosis (staurosporine; Fig. 3E).

For comparison, we tested the effects of CoA4, a well-studied tubulin-depolymerizing and vascular-disrupting drug, on endothelial cells. Fig. 2D summarizes and compares the effect of CoA4 on HMEC-1 proliferation, migration, vessel formation and attachment to ECM. CoA4 had qualitatively similar effects to those of JG-03-14, having somewhat more potent inhibitory effects on cell attachment and proliferation. Interestingly, while the two drugs had quantitatively similar effects on *in vitro* microvessel formation (IC_{50}s of 40 and 50 nM for JG-03-14 and CoA4, respectively), the latter drug was substantially more efficient in inhibiting cell migration than was JG-03-14 (130 nM vs. 50 nM, respectively). These data suggest that like other microtubule-binding agents, JG-03-14 has several anti-vascular effects that are observed *in vitro* at concentrations much lower than those affecting cell survival or proliferation.

3.3. JG-03-14 induces endothelial cell retraction, intercellular gaps, and plasma membrane blebbing

The effect of JG-03-14 on the morphology and cytoskeleton of EC is shown in the lower panel of Fig. 3. Cultures treated with a concentration of JG-03-14 that substantially blocked cell migration and tube formation (100 nM for 24 h; panels L & Q) show two distinct morphological changes. The majority of the cells showed varying but modest degrees of retraction and rounding, with no dramatic changes in the arrangement or amount of F-actin or microtubules observed. In contrast, a minority (15–20%) of the cells acquired a denser, more rounded morphology, and many of these cells appeared to be cycle-arrested at metaphase/anaphase (arrow in Fig. 3L).

Pharmacokinetic studies of CoA4 have shown that upon administration by a short infusion, it initially attains plasma concentrations in the micromolar range [29]. Subsequent drug distribution and/or elimination cause drug plasma levels to rapidly

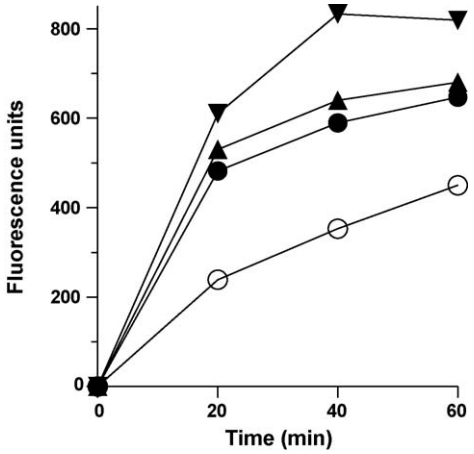

Fig. 4. JG-03-14 increases the permeability of an endothelial cell layer. Confluent HMEC-1 were grown on transwell filters to confluency in the upper well of a Boyden chamber. They were then treated with 100 nM JG-03-14 (●), combretastatin A4 (▲), colchicine (▼), or no drug (○) for 24 h. FITC-dextran was then added to the upper chambers. Passage of the FITC-dextran into the lower chambers was monitored at the indicated time intervals up to 1 h.

drop into the nanomolar range, usually within 1–2 h after the completion of drug administration. We therefore examined the effect of brief (1.5 h) treatment with micromolar concentrations of JG-03-14 on endothelial cell morphology and the cytoskeleton (Fig. 3M, N, R and S). The majority of the endothelial cells treated with 1 μM or 20 μM cells showed distinctive plasma membrane blebs (green and red arrows), defined as dynamic cytoskeleton-regulated cell protrusions that have been implicated in apoptosis, cytokinesis, and cell movement [30]. The cells were also more rounded than control cells, and typically had a dense band of F-actin just inside of the plasma membrane. These changes occurred after only 15 min of drug treatment (not shown), and were similar to those reported for CoA4 and nocodazole [31,32]. Surprisingly, two different types of blebs were observed. Some blebs were constituted by F-actin (red arrows in 3N), while others appeared to be filled with tubulin (green arrows in 3M and 3N); the merged images show very little overlapping of the two types of blebs. The tubulin blebs were larger than the F-actin blebs, and they also were observed earlier in response to the drug (not shown). Interestingly, the blebbing induced by JG-03-14 is reversible, since when the drug is removed the cells recover their normal morphology and actin stress fibers reform (Fig. 3O and T), with an apparent reversal of the cell cycle arrest as well.

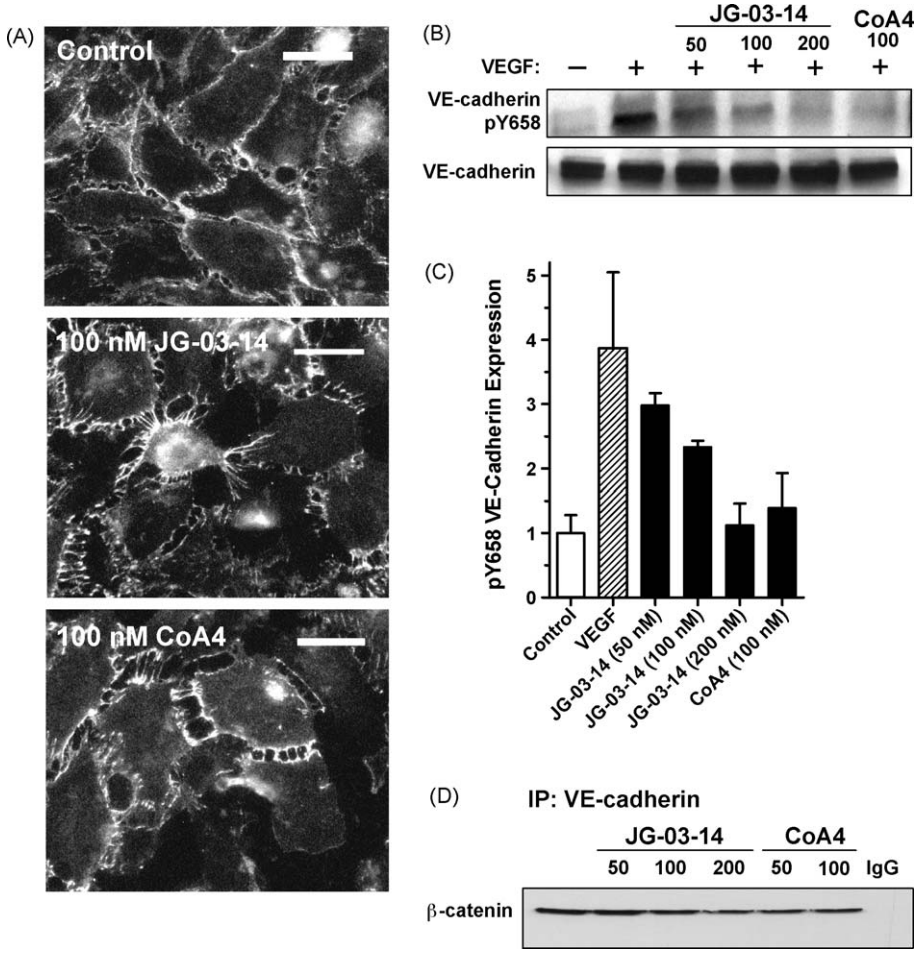

Fig. 5. JG-03-14 disrupts endothelial cell-cell interactions, reduces the level of phospho-VE-cadherin, and disrupts the VE-cadherin/β-catenin complex. (A) Confluent HMEC-1 cells were treated for 24 h with 100 nM JG-03-14 or with 100 nM CoA4, as indicated, followed by VEGF (10 ng/ml) for 15 min. The cultures were fixed and assayed by immunofluorescence with anti-VE-cadherin. Bar = 20 μm. (B. and C) HMEC-1 cells were incubated with the indicated nM concentrations of JG-03-14 or CoA4 for 24 h, followed by VEGF for 15 min. Panel (B) is a Western blot probed with anti-phosphotyrosine–VE-cadherin or for total VE-cadherin. Quantitation of the intensity of the bands is shown in panel (C) and is an average of two independent experiments. (D) HMEC-1 cells were incubated with the indicated concentrations of JG-03-14 or CoA4 for 24 h. After drug treatment the HMEC-1 cells were lysed and the extracts were immunoprecipitated with a rabbit anti-VE-cadherin antibody or as a negative control, rabbit IgG. Immunoprecipitated proteins were assayed by western blot with mouse anti-β-catenin.

A method to quantify the functional effect of drug-induced cell contraction and other morphological changes is to determine if there is an increase in intercellular gap formation by measuring the permeability of the cell monolayer to macromolecules. A similar increase in gap formation occurring *in vivo* would likely lead to increases in the leakiness of the vasculature. Fig. 4 shows that confluent endothelial cell cultures treated with 100 nM JG-03-14 for 24 h had higher permeability to FITC-dextran than did control cultures. Comparisons with other microtubule-depolymerizing drugs were done, and Fig. 4 shows that the effect of JG-03-14 was equivalent to that of 100 nM CoA4, and that these two drugs were somewhat less active than colchicine.

3.4. JG-03-14 causes abnormally elongated adherent junctions, reduces VE-cadherin phosphorylation, and disrupts the VE-cadherin/β-catenin complex

The endothelial cell-specific transmembrane adhesion protein VE-cadherin is critical to the formation and maintenance of the neovasculature, and it contributes to endothelial cell migration, survival, vascular integrity, and of particular relevance to the present study, the assembly of endothelial cells into tube-like structures [9,14]. VE-cadherin stabilizes cell–cell interactions at structures called adherens junctions, acting though the homophilic binding of its extracellular domain and the interaction of its cytoplasmic region with actin. In control endothelial cells, VE-cadherin is present along the cell periphery at well organized and distributed junction points between adjacent cells (Fig. 5A). In contrast, on drug treated cells (JG-03-14 and CoA4), VE-cadherin is localized on structures that appear stretched between the cells; the formation of these structures may have occurred when the cells contracted from their junction points (Fig. 5A). These structures appear particularly abnormally elongated in the JG-03-14-treated cells, where they extend in some instances up to 5–8 μm in length.

VE-cadherin contains nine tyrosine residues, and these are mainly unphosphorylated in quiescent vessels and in confluent endothelial cell cultures [33,34]. VEGF and other migration stimuli rapidly induce the phosphorylation of VE-cadherin, and this triggers the modification of the adherens junction that is thought to allow for the orderly loosening of cell–cell contacts that would be required for the sprouting of a new vessel [35]. JG-03-14 abrogated the VEGF-induced increase in VE-cadherin phosphorylation at tyrosine-658 without affecting the cellular levels of total VE-cadherin (Fig. 5B and C). The linkage of the cytoplasmic region of VE-cadherin with the actin cytoskeleton is mediated by a number of proteins, including α- and β-catenin, p120, and plakoglobin, and their interactions with VE-cadherin tend to strengthen adherens junctions. Using a co-immunoprecipitation assay, JG-03-14 was observed to reduce the interaction of VE-cadherin with a key component of the adherens junction, β-catenin (Fig. 5D). While de-phosphorylation of VE-cadherin and reduction in its reversible interaction with the catenins are part of the dynamic process by which adherens junctions are regulated, the abnormal VE-cadherin structures seen in JG-03-14-treated cells suggest that the drug-induced effects are preventing the normal functioning of VE-cadherin to mediate cell–cell interaction.

3.5. JG-03-14 does not interfere with VEGF-induced focal adhesion formation or with focal adhesion kinase (FAK) phosphorylation in endothelial cells

As shown above, JG-03-14 inhibits endothelial cell migration, a coordinated process that involves the formation of new EC-ECM adhesion sites called focal adhesions. Along with the integrins and growth factor receptors, including those for VEGF, a critical component of focal adhesions is focal adhesion kinase (FAK), a tyrosine kinase that links ECM proteins to intracellular actin filaments, and regulates cell shape, formation of cell protrusions, cell adhesion and cell motility [36]. Since other microtubule-binding drugs have been previously found to block the formation of focal adhesions and the autophosphorylation of FAK [37,38], we examined if JG-03-14, CoA4 and colchicine had similar effects. VEGF increased the number and size of the focal adhesions in HMEC-1 cells, and surprisingly, rather than inhibiting focal adhesion formation, JG-03-14 further increased the number and staining intensity of focal adhesions found along the periphery of the cells (Fig. 6A). While unexpected, this observation is consistent with the increase in cell adhesion produced by JG-03-14 (Fig. 2C). VEGF also induced a rapid increase in FAK phosphorylation at the tyrosine-379 autophosphorylation site, and this increase was not altered by JG-03-14, CoA4, or colchicine (Fig. 6B). Consistent with

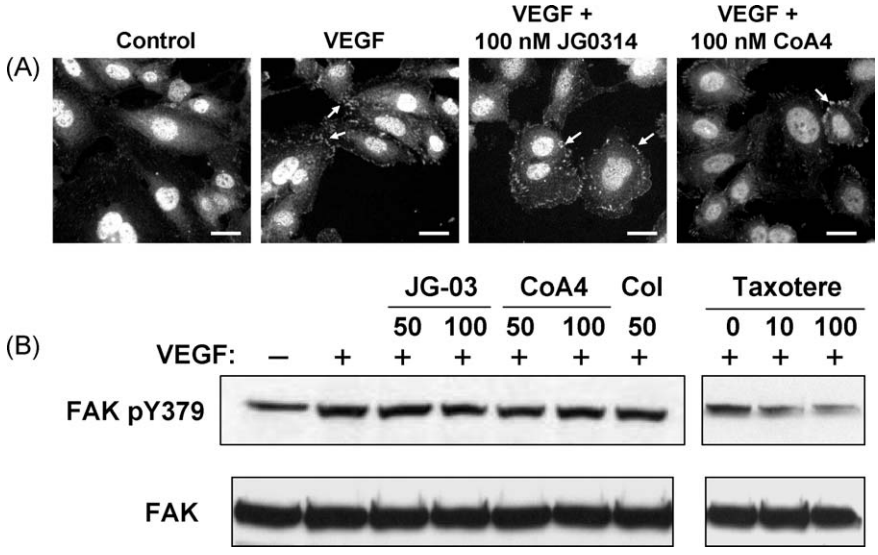

Fig. 6. JG-03-14 does not reduce focal adhesion density or interfere with activation of focal adhesion kinase (FAK). HMEC-1 cells were incubated with the indicated concentrations of JG-03-14, CoA4 and colchicine (Col) or taxotere for 24 h, followed by the addition of VEGF (10 ng/ml) for 15 min. (A) Immunofluorescence with anti-FAK antibody. Arrows indicate focal adhesions; bar = 20 μm. (B) Western blotting with anti-phosphotyrosine^{379} FAK or total FAK antibodies.

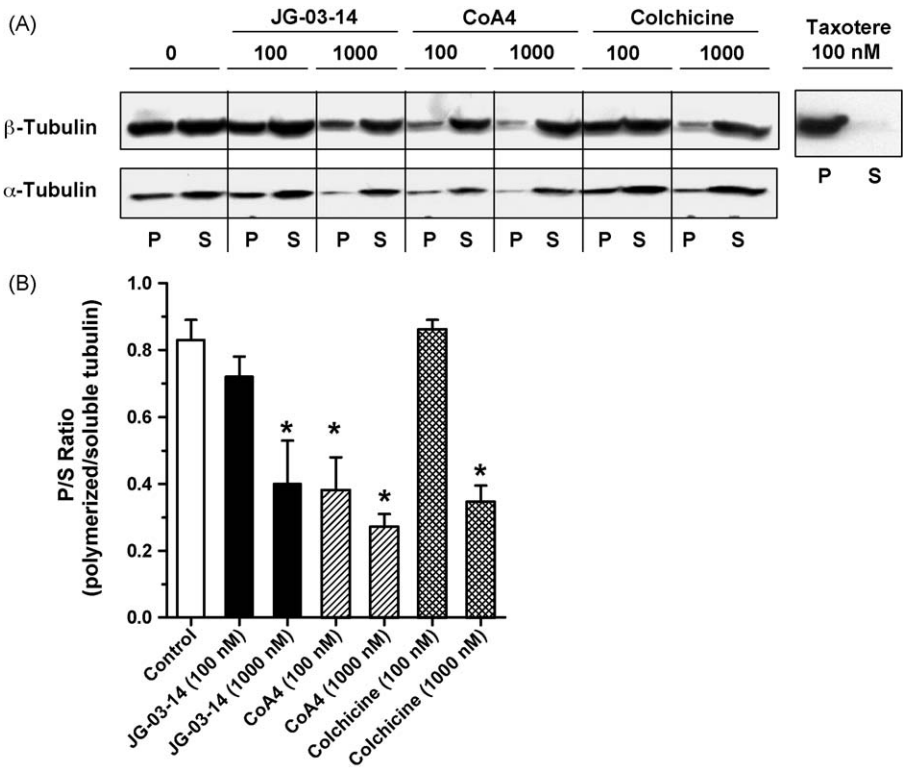

Fig. 7. JG-03-14 does not disrupt endothelial cell microtubule polymerization at concentrations which inhibit migration and tube formation. (A) Western blotting analysis of soluble (S) and polymerized (P) tubulin fractions, which were separated as described in Section 2 from HMEC-1 cells treated with 100 nM and 1000 nM of JG-03-14, colchicine or combretastatin A4 (CoA4) for 2 h. The blot was probed with anti-β-tubulin or anti-α-tubulin antibodies. The right panel is from cells treated with 100 nM taxotere, which causes microtubule stabilization. (B) Quantification of the relative intensity of the β-tubulin bands in panel A, presented as the ratio of polymerized to soluble tubulin (P/S). Data are means ± SEM of 3 independent experiments. *Indicates significantly different from control, $P < 0.05$, by ANOVA with Tukey's multiple comparison test.

an earlier report [37], the VEGF-induced increase in FAK phosphorylation was found to be completely blocked by taxotere (Fig. 6B).

3.6. JG-03-14 does not disrupt endothelial microtubule polymerization at drug concentrations which inhibited tube formation

Agents which bind to the colchicine site on tubulin inhibit the assembly of tubulin into microtubules, with a consequent cellular loss of polymerized microtubules. JG-03-14 has this effect on microtubules in cell-free systems, although the loss of interphase microtubules has only been observed in intact cells at drug concentrations of 250 nM and higher [24]. We did not observe any apparent effect of 100 nM JG-03-14 on microtubules in interphase endothelial cells, as judged by immunofluorescence (Fig. 3C and F). To confirm these observations, a differential extraction procedure to separate polymerized from soluble tubulin was used. In control cells, approximately 45% of cellular tubulin is polymerized and insoluble in this assay, and this ratio is not significantly different in HMEC-1 cells treated with 100 nM JG-03-14 for 2 h, conditions in which it substantially inhibited vessel formation (Fig. 7A and B). The validity of the assay was confirmed by the observations that a higher concentration of JG-03-14 (1000 nM) caused a significant loss of polymerized tubulin, and by the fact that taxotere, a microtubule stabilizing agent, produced the anticipated effect on the tubulin P/S ratio (Fig. 7A and B). Interestingly, colchicine had a comparable effect on the tubulin P/S ratio as did JG-03-14 while CoA4 did not, causing a significant depolymerization at a concentration of 100 nM. Whether these differences contribute to the variations in the range of anti-vascular effects for each agent remains to be determined. These data strongly suggest, however, that an effect on microtubule polymerization is not required for some of the anti-vascular actions of JG-03-14.

4. Discussion

Previous studies in cancer cells have shown that JG-03-14 causes a concentration-dependent loss of cellular microtubules, the formation of aberrant mitotic spindles, accumulation of cells in the G2/M phase of the cell cycle, Bcl-2 phosphorylation, and autophagy and apoptosis in breast cancer cells [24,25]. In the present report, we find that JG-03-14 selectively inhibits the organization of endothelial cells into vessel-like tubes, disrupts established endothelial cell tubes, causes cell rounding and blebbing, and increases the permeability of a cell monolayer. These actions are consistent with both anti-angiogenic and vascular-disrupting effects; most other microtubule-binding drugs have been found to also possess one or both of these properties [39].

The effects of JG-03-14 on cell morphology were determined after treatment at both high concentrations for brief periods, and with lower concentrations for longer periods. Taken together, these two conditions would mimic the typical exposure of endothelial cells to anti-vascular drugs *in vivo* [29]. Many of the cells treated with JG-03-14 at 100 nM exhibited cell retraction and rounding, with little effect on the cytoskeleton. A more prominent morphological change that was observed in EC treated with 1–20 μM JG-03-14 was the appearance of plasma membrane blebs. Blebbing is caused by the cell's internal hydrostatic pressure in local regions where there is a disruption of the membrane–actin cortex interaction [30,40]. Although membrane blebbing is seen in cells undergoing apoptosis, it is also a feature in other physiological

processes, particularly in embryonic development, migration and cytokinesis in normal and tumor cells [30,40]. Blebbing, whether occurring physiologically or in response to CoA4 or nocodazole, is dependent on the myosin-driven contraction of actinomysin and the actin cortex, processes that are downstream of the small GTPase RhoA, the Rho-associated kinase ROCK, and p38 MAPK [30–32,40]. Similar to the blebbing observed with JG-03-14, studies have suggested that the rapid membrane blebbing observed with CoA4 or nocodazole treatment was reversible and mechanistically different from apoptotic blebbing [31,32].

The morphological and functional changes in endothelial cells caused by the combretastatins *in vitro* are thought to be related to the rapid collapse of the tumor vasculature and reduction in tumor blood flow these agents cause *in vivo* [10]. Endothelial cell rounding and blebbing would lead to a direct increase in the geometric resistance to blood flow, while an increase in vasculature permeability would allow the leakage of plasma proteins from the vasculature, thereby increasing the interstitial fluid pressure and reducing the oncotic pressure difference between the inside and outside of the vessel [41–43]. The rapidity with which this was observed in animal models and in clinical trials is likely due to the high plasma drug concentrations that occur immediately upon drug administration. More importantly, it is likely not due to drug-induced effects on EC proliferation and/or EC apoptosis, which occur too slowly to account for these anti-vascular actions.

It is important to consider the relationship between JG-03-14's cytotoxic actions and its effects on cell proliferation, with its ability to inhibit cell migration and vessel formation. As shown in Fig. 2, JG-03-14 inhibited EC vessel formation at concentrations that were 6-fold lower than required to inhibit proliferation and which did not activate cell death mechanisms, implying that non-specific cytotoxicity does not play a role in the drug's effect on vessel formation. This is consistent with other reports of the effects of microtubule-binding drugs [39]; for example, while colchicine and nocodazole did inhibit endothelial cell proliferation and induce apoptosis, they did so at concentrations 2-fold to 62-fold higher than required to inhibit *in vitro* angiogenesis [44]. This is in contrast to the actions of bleomycin and mitomycin C, which inhibited cell proliferation and induced endothelial cell apoptosis at concentrations equal to or 100-fold *lower* than required to inhibit *in vitro* angiogenesis [44]. If the anti-angiogenic effects of the microtubule-binding drugs were solely due to cytotoxicity, bleomycin and mitomycin C would be expected to be equal in activity as angiogenesis inhibitors as were colchicine and nocodazole, but they were not.

EC vessel formation *in vitro* does not in fact require cell proliferation; indeed untreated endothelial cells become quiescent when plated on Matrigel and do not undergo cell division [11]. Interestingly, although time-lapse microscopy has shown that capillary vessel network formation involves cell migration, the effect of JG-03-14 on vessel formation occurred at 3-fold lower concentrations than its inhibitory effect on cell migration [45]. This suggests that inhibition of cell motility was not the sole mechanism by which JG-03-14 blocked vessel formation. This is in contrast to CoA4, where the inhibition curves for cell migration and vessel formation essentially overlapped; like JG-03-14, inhibition of migration and vessel formation occurred at concentrations that were lower of CoA4 than were required to inhibit proliferation [45]. Also in contrast to CoA4, it is noteworthy that JG-03-14 did not cause a loss in cellular polymerized microtubules at concentrations that completely inhibited vessel formation.

These observations suggest that the nature of the interaction of a particular small molecule with the colchicine binding site on tubulin can influence the cellular effects observed. Whether these differences observed in tissue culture translate into therapeutically relevant anti-angiogenic and vascular-disrupting actions remains to be determined. In this regard JG-03-14 may be a particularly valuable starting point for future studies, since in contrast to the combretastatins, its pyrrole scaffold is readily amenable to chemical manipulation and analog synthesis, providing a basis for future studies into structure-activity relationships to better define the relationship between microtubule binding and anti-vascular activity [46].

Similar to CoA4, JG-03-14 appears to disrupt the adherens junctions and inhibit VE-cadherin phosphorylation [45]. Given the critical role cell–cell interactions play in tube formation and maintenance, the effect of JG-03-14 on VE-cadherin could account for many of the effects observed in this study. In support of this is direct evidence showing that tube formation on ECM was inhibited by antibodies to VE-cadherin, but not by antibodies to N-cadherin, integrin $\alpha_v\beta_3$, or PECAM-1 [9,45]. Other studies found that while an anti-integrin $\alpha_v\beta_3$ antibody did not block the ability of ECs to initially form a tubular network on Matrigel, it did cause the subsequent dissolution of the network. Integrins are cell adhesion molecules that form focal adhesions and thereby mediate cell–ECM interactions; thus the hindrance of either focal adhesion or adherens junction function can lead to capillary vessel disruption. The fact that JG-03-14 did not inhibit focal adhesion formation or FAK phosphorylation suggests its primary action was on the adherens junction. Remarkably, the effect of JG-03-14 was opposite to that of the microtubule-binding taxanes, which have been reported to reduce focal adhesion formation, inhibit FAK phosphorylation, and block integrin activation and signaling [37,38]. The fact that microtubule-stabilizing and destabilizing agents target different adhesion molecules on endothelial cells provides a compelling rationale for the use of combinations of these two classes of agents for their potential complementary anti-vascular actions.

Acknowledgment

We thank Rachel Hazan for helpful discussions.

References

[1] Jordan MA, Wilson L. Microtubules as a target for anticancer drugs. Nat Rev Cancer 2004;4:253–65.
[2] Belotti D, Vergani V, Drudis T, Borsotti P, Pitelli MR, Viale G, et al. The microtubule-affecting drug paclitaxel has antiangiogenic activity. Clin Cancer Res 1996;2:1843–9.
[3] Dark GG, Hill SA, Prise VE, Tozer GM, Pettit GR, Chaplin DJ. Combretastatin A-4, an agent that displays potent and selective toxicity toward tumor vasculature. Cancer Res 1997;57:1829–34.
[4] Klauber N, Parangi S, Flynn E, Hamel E, D'Amato RJ. Inhibition of angiogenesis and breast cancer in mice by the microtubule inhibitors 2-methoxyestradiol and taxol. Cancer Res 1997;57:81–6.
[5] Vacca A, Iuralaro M, Ribatti D, Minschetti M, Nico B, Ria R, et al. Antiangiogenesis is produced by nontoxic doses of vinblastine. Blood 1999;94:4143–55.
[6] Hotchkiss KA, Ashton AW, Mahmood R, Russell RG, Sparano JA, Schwartz EL. Inhibition of endothelial cell function *in vitro* and angiogenesis *in vivo* by docetaxel (taxotere): association with impaired repositioning of the microtubule organizing center. Mol Cancer Ther 2002;1:1191–200.
[7] Grant DS, Williams TL, Zahaczewsky M, Dicker AP. Comparison of the anti-angiogenic activities using paclitaxel (taxol) and docetaxel (taxotere). Int J Cancer 2003;104:121–9.
[8] Stafford SJ, Schwimer J, Anthony CT, Thomson JL, Wang YZ, Woltering EA. Colchicine and 2-methoxyestradiol inhibit human angiogenesis. J Surg Res 2005;125:104–8.
[9] Bach TL, Barsigian C, Chalupowicz DG, Busler D, Yaen CH, Grant DS, et al. VE-cadherin mediates endothelial cell capillary tube formation in fibrin and collagen gels. Exptl Cell Res 1998;238:324–34.
[10] Tozer GM, Kanthou C, Baguley BC. Disrupting tumour blood vessels. Nat Rev Cancer 2005;5:423–35.
[11] Kubota Y, Kleinman HK, Martin GR, Lawley TJ. Role of laminin and basement membrane in the morphological differentiation of human endothelial cells into capillary-like structures. J Cell Biol 1988;107:1589–98.
[12] Pollman MJ, Maumovski L, Gibbons GH. Endothelial cell apoptosis in capillary network remodeling. J Cell Physiol 1999;178:359–70.

[13] Stromblad S, Cheresh DA. Cell adhesion and angiogenesis. Trends Cell Biol 1996;6:462–8.
[14] Vestweber D. VE-cadherin. The major endothelial adhesion molecule controlling cellular junctions and blood vessel formation. Arterioscler Thromb Vasc Biol 2008;28:223–32.
[15] Skoulias D, Wilson L. Mechanism of inhibition of microtubule polymerization by colchicine: inhibitory potencies of unliganded colchicine and tubulin-colchicine complexes. Biochemistry 1992;31:738–46.
[16] Waterman-Storer CM, Salmon ED. Positive feedback interactions between microtubule and actin dynamics during cell motility. Curr Opin Cell Biol 1999;11:61–7.
[17] Goldman RD. The role of three cytoplasmic fibers in BHK-12 cell motility. I. Microtubules and the effect of colchicine. J Cell Biol 1971;51:752–62.
[18] Lin CM, Singh SB, Chu PS, Dempcy RO, Schmidt JM, Pettit GR, et al. Interactions of tubulin with potent natural and synthetic analogs of the antimitotic agent combretastatin: a structure-activity study. Mol Pharmacol 1988;34:200–8.
[19] Hamel E, Lin CM, Flynn E, D'Amato RJ. Interactions of 2-methoxyestradiol, an endogenous mammalian metabolite, with unpolymerized tubulin and with tubulin polymers. Biochemistry 1996;35:1304–10.
[20] Yoshimatsu K, Yamaguchi A, Yoshino H, Koyanagi N, Kitoh K. Mechanism of action of E7010, an orally active sulfonamide antitumor agent: inhibition of mitosis by binding to the colchicine site of tubulin. Cancer Res 1997;57: 3208–13.
[21] Mooberry SL. New insights into 2-methoxyestradiol, a promising antiangiogenic and antitumor agent. Curr Opin Oncol 2003;15:425–30.
[22] Gupton J, Burham B, Krumpe K, Du K, Sikorski J, Warren A. Synthesis and cytotoxicity of 2,4-disubstituted and 2,3,4-trisubsitituted brominated pyrroles in murine and human cultured tumor cells. Arch Pharm 2000; 333:3–9.
[23] Gupton JT. Pyrrole natural products with antitumor properties. In: Lee M, editor. Heterocyclic Antitumor Antibiotics: Topics in Heterocyclic Chemistry. Berlin: Springer–Verlag; 2006. p. 53–92.
[24] Mooberry SL, Weiderhold KN, Dakshanamurthy S, Hamel E, Banner EJ, Kharlamova A, et al. Identification and characterization of a new tubulin-binding tetrasubstituted brominated pyrrole. Mol Pharmacol 2007;72:132–40.
[25] Arthur CR, Gupton JT, Kellogg GE, Yeudal WA, Cabot MC, Newsham IF, et al. Autophagic cell death, polyploidy and senescence induced in breast tumor cells by the substituted pyrrole JG-03-14, a novel microtubule poison. Biochem Pharmacol 2007;74:981–91.
[26] Ades EW, Candal FJ, Swerlick RA, George VG, Summers S, Bosse DC, et al. HMEC-1: establishment of an immortalized human microvascular endothelial cell line. J Invest Dermatol 1992;99:683–90.
[27] Lieuvin A, Labbé J-C, Dorée M, Job D. Intrinsic microtubule stability in interphase cells. J Cell Biol 1994;124:85–996.
[28] Bershadsky AD, Gelfand VI, Svitkina TP, Tint IS. Microtubules in mouse embryo fibroblasts extracted with Triton X-100. Cell Biol Intern Rep 1978;2:425–32.
[29] Rustin GJ, Galbraith SM, Anderson H, Stratford M, Folkes LK, Sena L, et al. Phase I clinical trial of weekly combretastatin A4 phosphate: clinical and pharmacokinetic results. J Clin Oncol 2003;21:2815–22.
[30] Fackler OT, Grosse R. Cell motility through plasma membrane blebbing. J Cell Biol 2008;181:878–84.
[31] Kanthou C, Tozer GM. The tumor vascular targeting agent combretastatin A-4-phosphate induces reorganization of the actin cytoskeleton and early membrane blebbing in human endothelial cells. Blood 2002;99:2060–9.
[32] Jia Z, Vadnais J, Lu ML, Noel J, Nabi IR. Rho/ROCK-dependent pseudopodial protrusion and cellular blebbing are regulated by p38 MAPK in tumour cells exhibiting c-Met activation. Biol Cell 2006;98:337–51.
[33] Lampugnani MG, Corada M, Andriopoulou P, Esser S, Risau W, Dejana E. Cell confluence regulates tyrosine phosphorylation of adherens junction components in endothelial cells. J Cell Sci 1997;110:2065–77.
[34] Wallez Y, Vilgrain I, Huber P. Angiogenesis: the VE-cadherin switch. Trends Cardiovasc Med 2006;16:55–9.
[35] Esser S, Lampugnani MG, Corada M, Dejana E, Risau W. Vascular endothelial growth factor induces VE-cadherin tyrosine phosphorylation in endothelial cells. J Cell Sci 1998;111:1853–65.
[36] Mitra SJ, Hanson DA, Schlaepfer DD. Focal adhesion kinase: in command and control of cell motility. Nat Rev Mol Cell Biol 2005;6:56–68.
[37] Lu H, Murtagh J, Schwartz EL. The microtubule binding drug laulimalide inhibits vascular endothelial growth factor-induced human endothelial cell migration and is synergistic when combined with docetaxel (taxotere). Mol Pharmacol 2006;69:1207–15.
[38] Murtagh J, Lu H, Schwartz EL. Taxotere-induced inhibition of human endothelial cell migration is a result of heat shock protein 90 degradation. Cancer Res 2006;66:8192–9.
[39] Schwartz EL. Antivascular actions of microtubule-binding drugs. Clin Cancer Res 2009;15:2594–601.
[40] Charras G, Paluch E. Blebs lead the way: how to migrate without lamellipodia. Nat Rev Mol Cell Biol 2008;9:730–6.
[41] Milosevic MF, Fyles AW, Hill RP. The relationship between elevated interstitial fluid pressure and blood flow in tumors: a bioengineering analysis. Int J Radiat Oncol Biol Phys 1999;43:1111–23.
[42] Tozer GM, Prise VE, Wilson J, Cemazar M, Shan S, Dewhirst MW, et al. Mechanisms associated with tumor vascular shut-down induced by combretastatin A-4 phosphate: intravital microscopy and measurement of vascular permeability. Cancer Res 2001;61:6413–22.
[43] Blakey DC, Westwood FR, Walker M, Hughes GD, Davis PD, Ashton SE, et al. Antitumor activity of the novel vascular targeting agent ZD6126 in a panel of tumor models. Clin Cancer Res 2002;8:1974–83.
[44] Mabeta P, Pepper MS. A comparative study on the anti-angiogenic effects of DNA-damaging and cytoskeletal-disrupting agents. Angiogenesis 2009;12: 81–90.
[45] Vincent L, Kermani P, Young LM, Cheng J, Zhang F, Shido K, et al. Combretastatin A4 phosphate induces rapid regression of tumor neovessels and growth through interference with vascular endothelial-cadherin signaling. J Clin Invest 2005;115:2992–3006.
[46] Tripathi A, Fornabaio M, Kellogg GE, Gupton JT, Gewirtz DA, Yeudall WA, et al. Docking and hydropathic scoring of polysubstituted pyrrole compounds with antitubulin activity. Bioorg Med Chem 2008;16:2235–42.